J. Fluid Mech. (1987), *vol.* 179, *pp.* 513–529
Printed in Great Britain

On the breakdown of the steady and unsteady interacting boundary-layer description

By R. A. W. M. HENKES
Department of Applied Physics, Delft University of Technology,
P.O. Box 356, Delft, The Netherlands

AND A. E. P. VELDMAN
Department of Mathematics and Informatics, Delft University of Technology,
P.O. Box 356, Delft, *and* National Aerospace Laboratory NLR,
P.O. Box 90502, Amsterdam, The Netherlands

(Received 24 April 1986)

It is known that the classical boundary-layer solution breaks down through the appearance of the Goldstein singularity in a steady solution or Van Dommelen's singularity in an unsteady solution. Interaction between the inviscid flow and the boundary layer removes the Goldstein singularity, until a new critical parameter is reached, corresponding to a marginal separation in the asymptotic triple-deck description. In earlier studies instabilities were encountered in interacting boundary-layer calculations of steady flow along an indented plate, which might be related to the breakdown of the marginal separation. The present study identifies them as numerical. Further, until now it was unknown whether the unsteady interacting boundary-layer approach would remove Van Dommelen's singularity in the classical boundary layer around an impulsively started cylinder. It is shown here that its appearance is at least delayed. The calculations show the experimentally known individualization of a vortex, after which the solution grows without reaching a steady limit; a process that is likely to be related to dynamic stall.

1. Introduction

When one relies on the physics to select initial and boundary conditions, the Navier–Stokes equations are expected to give a complete mathematical description of the flow. For large Reynolds numbers the Navier–Stokes solution can be approximated by an asymptotic description. Critical combinations of parameters (e.g. angle of incidence, geometry size, Reynolds number) can exist where a certain asymptotic description fails to represent the physics and breaks down. This mathematical breakdown can be characterized by a singularity, the non-existence/non-uniqueness of the steady solution, or the growth beyond all bounds at infinitely large time of the unsteady solution. In the worst case the asymptotic solution may diverge from the Navier–Stokes solution without a special warning. The breakdown indicates the need to introduce new asymptotic equations to continue the asymptotic description of the Navier–Stokes solution. The large effort required to calculate a high-Reynolds-number Navier–Stokes solution, owing to the existence of different time- and lengthscales, motivates the search for these new asymptotic structures. Another reason to continue studying asymptotic descriptions is its great physical relevance. A breakdown might be related to the transition to another

physical structure: the breaking away of the boundary layer from the wall, the formation of a vortex, or the dynamic stall process.

The classical asymptotic description of Prandtl (1904) omits the viscous terms everywhere, yielding the Euler equations, except in a thin layer along the wall, where the (classical) boundary-layer equations hold. Goldstein (1948) proved that the steady classical boundary-layer solution, in which the pressure is prescribed, has a singularity at the point of zero wall shear stress, unless the pressure satisfies some special conditions. Van Dommelen (1981) calculated the appearance of a singularity, not of the Goldstein type, in the unsteady classical boundary-layer solution within a finite time after the impulsive start of a cylinder. Sychev (1972) and Smith (1977, 1979) removed the Goldstein singularity in the steady solution by the introduction of the triple-deck equations in the neighbourhood of the point of zero wall shear stress; the pressure is no longer prescribed but results from interaction with the boundary layer. Sychev showed that the triple-deck description is consistent with the assumption that the Kirchhoff free-streamline solution is the relevant Euler solution for the cylinder (Brodetski 1923); triple-deck equations describe finite-Reynolds-number effects in the neighbourhood of the position where the free streamline leaves the wall (at 56°). This description, in which the boundary layer is continued as a free shear layer along the free streamline, agrees with Prandtl's suggestion that a large-scale breaking away of the boundary layer, i.e. the 'separation' of the boundary layer, is found in the steady flow when the wall shear stress vanishes. Stewartson, Smith & Kaups (1982) describe it as the transition from an 'attached' boundary layer (viscous effects are only felt in an $O(R^{-\frac{1}{2}})$ layer close to the wall) to a 'detached' boundary layer (viscous effects are also felt in layers further removed from the wall). Separation, attachment and detachment are defined here within the boundary-layer concept of asymptotically large Reynolds numbers, indicating that a free shear layer leaves the wall. Frequently, the same terms are also used within the real (Navier–Stokes) concept for finite Reynolds numbers, describing a streamline leaving the wall. This can easily lead to confusion.

A singularity in the classical boundary layer does not necessarily imply its large-scale breaking away; finite-Reynolds-number viscous–inviscid interaction can prevent it, admitting a small recirculation region (bubble) in the steady boundary layer, but leaving it still attached. Considering triple-deck equations, Stewartson *et al.* (1982) reserve the terms 'marginal separation' for this behaviour. Within this asymptotic framework, calculations of boundary layers with recirculation have already been performed. Dijkstra (1979) calculated a steady boundary layer, with bubble, along a wall with a smooth step, using triple-deck equations. In the same way, the bubble along an indented plate was calculated (Veldman & Dijkstra 1980). Both geometries fit the triple-deck scalings; hence in the limit of infinite Reynolds number there is no bubble at all. Stewartson *et al.* (1982) used the same equations for a leading-edge bubble on a thin ellipse at an angle of incidence. From their calculations it follows that a critical combination of parameters (thickness ratio of the ellipse, angle of incidence and Reynolds number) exists, where non-existence or non-uniqueness of the solution occurs. Smith (1982) repeated the analysis with unsteady triple-deck equations for parameters where a steady triple-deck solution does not exist; rapidly growing peaks in the displacement thickness are calculated, corresponding to the formation of many eddies, strongly indicating the appearance of a finite-time singularity. Smith suggested that this behaviour is related to the dynamic-stall process, in which a small increase of the angle of incidence totally

changes the streamline pattern, achieving the violently unsteady transition from an attached to a detached boundary layer.

One might want to go one step further and calculate attached boundary layers with bubbles that do not fit into the asymptotic triple-deck scalings. Veldman (1979, 1981) generalized the triple-deck idea to a composite formulation, valid in the whole boundary layer, in which all asymptotic layers, whatever they may be, are hidden. Its unsteady formulation, in boundary-layer scalings, for two-dimensional, isothermal, incompressible, laminar flows, is

$$\left.\begin{aligned} \frac{\partial u}{\partial x}+\frac{\partial v}{\partial y} &= 0, \\ \frac{\partial u}{\partial t}+u\frac{\partial u}{\partial x}+v\frac{\partial u}{\partial y} &= -\frac{\partial p}{\partial x}+\frac{\partial^2 u}{\partial y^2}, \end{aligned}\right\} \tag{1}$$

with the initial and boundary conditions

$$\left.\begin{aligned} t=0: &\quad u, v \quad \text{components specified}, \\ y=0: &\quad u=v=0, \\ y\to\infty: &\quad u(x,y,t)\to u_e(x,t), \\ &\quad u_e(x,t)=u_{e,0}(x,t)+\frac{1}{\pi R^{\frac{1}{2}}}\oint_{x_b}^{x_e}\frac{\partial(u_e\delta^*)/\partial\xi}{x-\xi}\,\mathrm{d}\xi, \\ x=x_b: &\quad u\text{-profile (without backflow) of the oncoming boundary layer specified.} \end{aligned}\right\} \tag{2}$$

The displacement thickness δ^* is defined as

$$\delta^*(x,t)=\int_0^\infty\left(1-\frac{u(x,y,t)}{u_e(x,t)}\right)\mathrm{d}y. \tag{3}$$

The first part of the edge velocity, $u_{e,0}$, results from the Euler solution, assuming an attached vanishingly thin boundary layer. The second part, with the Cauchy integral, accounts for the viscous–inviscid interaction; only a simple interaction model is used representing the displacement effect on the potential solution of a distribution of sources on the straight line between x_b and x_e. The composite formulation (1) and (2) is referred to as the interacting boundary-layer equations. Its steady formulation was used by Carter & Wornom (1975), Veldman (1979, 1981) and Edwards & Carter (1985) to calculate the attached boundary layer, with bubble, along a plate with a small indentation. Convergence problems are revealed for very large Reynolds numbers, which could be related to non-existence or non-uniqueness of the solution, similar to the breakdown of the steady triple-deck solution according to Stewartson *et al.*

In the present paper the interacting boundary-layer equations are considered. We investigate whether a breakdown occurs, and if so, how it is related to the breakdown in the classical theories (Goldstein and Van Dommelen) and in the triple-deck theory (Stewartson *et al.* and Smith). Recently the interacting boundary-layer equations for a trailing-edge configuration were solved by Rothmayer & Davis (1985); the interacting boundary-layer solution in this case breaks down in a way similar to that of the triple-deck equations. Two new examples are given here. With an unsteady evolution, we investigate whether the convergence problems of the steady interacting

boundary-layer solution along the indented plate are related to a breakdown (finite-time singularity or unboundedness for $t \to \infty$ of the unsteady solution, implying the non-existence of the steady solution) or whether they have only a numerical cause. As a second example we consider a problem where the recirculation region is larger: we investigate the influence of interaction on Van Dommelen's finite-time singularity in the unsteady classical boundary-layer solution for the impulsively started cylinder.

2. Numerical procedure

All variables in (1) and (2) have been non-dimensionalized: time by l/U_0, lengths by l, velocities by U_0 and pressure by ρU_0^2. The Reynolds number is defined as

$$R = \frac{U_0 l}{\nu}. \tag{4}$$

The equations are reformulated with u, ψ variables. The stream function ψ is defined through

$$u = \frac{\partial \psi}{\partial y}, \quad v = -\frac{\partial \psi}{\partial x}. \tag{5}$$

The y-coordinate is rescaled with the outer edge $H(x,t)$ of the computational region,

$$\eta = \frac{y}{H(x,t)}. \tag{6}$$

Substitution of (5) and (6) into (1) and (2), and rewriting of the system as three first-order differential equations, by introduction of a scaled vorticity ω, gives

$$\frac{\partial \psi}{\partial \eta} - Hu = 0, \tag{7a}$$

$$H^2 \frac{\partial u}{\partial t} - \eta H \frac{\partial H}{\partial t}\omega + H^2 u \frac{\partial u}{\partial x} - H\frac{\partial \psi}{\partial x}\omega - H^2 \frac{\partial u_e}{\partial t} - H^2 u_e \frac{\partial u_e}{\partial x} - \frac{\partial \omega}{\partial \eta} = 0, \tag{7b}$$

$$\omega - \frac{\partial u}{\partial \eta} = 0, \tag{7c}$$

with the initial and boundary conditions

$$\left.\begin{aligned} &t = 0: \quad u, \psi, \omega \quad \text{variables specified,} \\ &\eta = 0: \quad u = \psi = 0, \\ &\eta = 1: \quad u(x,1,t) = u_e(x,t), \\ &\qquad u_e(x,t) = u_{e,0}(x,t) + \frac{1}{\pi R^2} \oint_{x_b}^{x_e} \frac{\frac{\partial}{\partial \xi}(H(\xi,t)\, u_e(\xi,t) - \psi_e(\xi,t))}{x - \xi} \mathrm{d}\xi, \\ &x = x_b: \quad u, \psi, \omega \text{ profiles of the oncoming bounding layer specified.} \end{aligned}\right\} \tag{8}$$

The computational region is covered by a grid (in space and time) with grid points (x_i, η_j, t_k), $(i = 1, 2, \ldots, I; j = 1, 2, \ldots, J; k = 1, 2, \ldots, K)$. The equations (7*a* and *c*) are discretized around the point $(x_i, \eta_{j-\frac{1}{2}}, t_k)$, whereas (7*b*) is discretized around $(x_i, \eta_{j-\frac{1}{2}}, t_{k-\frac{1}{2}})$ (Crank–Nicolson method). All derivatives on a station i are approximated with second-order accuracy using neighbouring grid points. In particular,

the convective term in the x-direction is discretized with grid points on the x-stations i, $i-1$ and $i-2$ in regions without backflow, and with grid points on the x-stations i, $i+1$ and $i+2$ in regions with backflow. This change of direction of discretization is required to prevent instabilities, which occur when the dependence rule (the numerical region of influence should enclose the analytical region of influence) with respect to the convection is not satisfied. In some unsteady evolutions to a steady solution the direction of discretization has to be frozen after a certain number of timesteps in order to avoid a limit cycle.

The Cauchy integral in the edge velocity is integrated by parts to replace the first-order pole in the integrand by a weaker singularity. At each time level the numerical integration of the integral is performed under the assumption that $\partial^2(u_e \delta^*)/\partial x^2$ is piecewise constant on intervals $[x_{i-\frac{1}{2}}, x_{i+\frac{1}{2}}]$ and that $\partial(u_e \delta^*)/\partial x = 0$ for $x \leqslant x_b$ and $x \geqslant x_e$. The result can be written as

$$\boldsymbol{u}_e = \boldsymbol{u}_{e,0} + \frac{1}{\pi R^{\frac{1}{2}}} \boldsymbol{P} \boldsymbol{u}_e \delta^*. \tag{9}$$

The matrix $\boldsymbol{P}$, considered except for its first row and column and its last row and column, turns out to be positive definite.

During each timestep a system of $(I-1) \times 3J$ nonlinear algebraic equations has to be solved. A combination of Gauss–Seidel and Newton–Raphson iterative procedures is used. Repeated Gauss–Seidel sweeps are made from station x_2 to x_I, in which the edge velocity iterates according to

$$u_{i,J}^{(n)} - \frac{1}{\pi R^{\frac{1}{2}}} p_{ii} A_i^{(n)} = (u_{e,0})_i + \sum_{l=1}^{i-1} \frac{1}{\pi R^{\frac{1}{2}}} p_{il} A_l^{(n)} + \sum_{l=i+1}^{I} \frac{1}{\pi R^{\frac{1}{2}}} p_{il} A_l^{(n-1)}, \quad i = 2, 3, \ldots, I, \tag{10}$$

with $A_i = (u_e \delta^*)_i = H_i u_{i,J} - \psi_{i,J}$, n = iteration level, p_{ij} = entry of the matrix $\boldsymbol{P}$.

The positive definite structure of $\boldsymbol{P}$ is a sufficient condition for the convergence of the Gauss–Seidel process. At each x-station a system of $3J$ nonlinear equations is solved with a Newton–Raphson process. The matrices appearing in this process have a sparse structure: block tridiagonal with an additional last block column (all 3×3 blocks).

The Gauss–Seidel iteration for the edge velocity (10), the so-called quasi-simultaneous method, was introduced by Veldman (1979, 1981) for the steady interacting boundary-layer equations. The quasi-simultaneous method prescribes a combination of u_e and δ^* in the Newton–Raphson process at each x-station: Prescription of u_e alone, the so-called direct method, gives, in the numerical process to solve the steady equations, a singular matrix as soon as backflow occurs, related to the Goldstein singularity. Prescription of δ^*, the so-called inverse method, in the numerical process to solve the steady interacting equations, is allowed, but its convergence is slower than that of the quasi-simultaneous method. Prescription of u_e in an unsteady evolution to a steady interacting boundary-layer solution does not lead to singular matrices, provided the timestep is small enough: Briley & McDonald (1975) marched through the computational region and prescribed the edge velocity explicitly at the new time level, updated with the displacement influence of the old time level. The present study uses the time-dependent approach together with the quasi-simultaneous method, because it has better stability properties, allowing larger timesteps than the direct method.

For further details about the numerical method used the reader is referred to Henkes (1985).

3. Indented plate

The shape of the indented plate, depicted in figure 1, is given (in boundary-layer coordinates) by

$$y_w = \alpha R^{\frac{1}{2}} \operatorname{sech} 4(x-2.5), \quad x \geqslant 0. \tag{11}$$

The Reynolds number (4) is based on the oncoming velocity u_∞ and the characteristic plate length l; α is taken as -0.03. The Euler solution, assuming an attached vanishingly thin boundary layer, is approximated by

$$u_{e,0} = 1 + \frac{1}{\pi R^{\frac{1}{2}}} \oint_0^\infty \frac{\mathrm{d}y_w/\mathrm{d}\xi}{x-\xi} \mathrm{d}\xi. \tag{12}$$

Calculated streamline patterns (previous results and new ones to be discussed next) are shown in figure 2.

The problem was originally defined by Carter & Wornom (1975) on the interval $1 \leqslant x \leqslant 4$. They presented solutions at a Reynolds number $R = 8 \times 10^4$. Veldman (1979, 1981) solved the problem at a Reynolds number $R = 3.6 \times 10^5$, but he could not obtain converged results for larger Reynolds numbers. Both investigations used interacting boundary-layer equations. Another approach was followed by Veldman & Dijkstra (1980). They treated the problem in a triple-deck framework, but they also encountered difficulties at Reynolds numbers slightly above 3.6×10^5. Careful iteration, using results at smaller Reynolds numbers as an initial guess, did not lead to success. Thus two different steady descriptions of the flow problem ran into difficulties in about the same situation. This gave the impression that something fundamental was going on: perhaps a steady solution does not exist at these large Reynolds numbers.

Recently, Edwards & Carter (1985) were able to calculate a steady solution at $R = 6 \times 10^5$, but they used a first-order scheme and they neglected the convective term in the x-direction in regions with backflow (FLARE approximation). Therefore we decided to give it another try. Using the first-order solution at $R = 6 \times 10^5$ as an initial guess, it appeared possible to obtain the steady solution with a second-order scheme, without neglect of any terms, at this Reynolds number.

Solutions at larger Reynolds numbers could only be obtained by following an unsteady approach, starting from the steady solution at $R = 6 \times 10^5$; the steady solution at $R = 1.5 \times 10^6$ was reached by increasing the Reynolds number as

$$R(t) = R_1 - (R_1 - R_0) \operatorname{sech}(t), \tag{13}$$

with $R_0 = 6 \times 10^5$, $R_1 = 1.5 \times 10^6$.

As a rule three sweeps were made at each time level. The almost steady solution on the 61×41 spatial grid at $t = 8.0$, after 75 timesteps, was used to initiate a calculation with the steady equations for $R = 1.5 \times 10^6$: another 58 sweeps were required to satisfy the criterion that the maximum norm of changes in $u_e \delta^*$ is below 10^{-4}.

The value $R = 1.5 \times 10^6$ was chosen such that the 61×41 numerical grid could resolve some of the details of the free shear layer; the wall shear stress in figure 3 between $x = 2.0$ and 2.5 already shows some 'wiggles' which are caused by a lack of resolution (all curves in this paper are found by just a linear interpolation between discrete numerical values). Larger Reynolds numbers would require a finer grid, with increased computational cost. The wiggle of $x = 1$ results from the interaction via the Cauchy integral which is suddenly switched on at $x = 1$. Calculations on coarser grids (31×21, 46×31) were made to confirm the accuracy of the curves in figure 3.

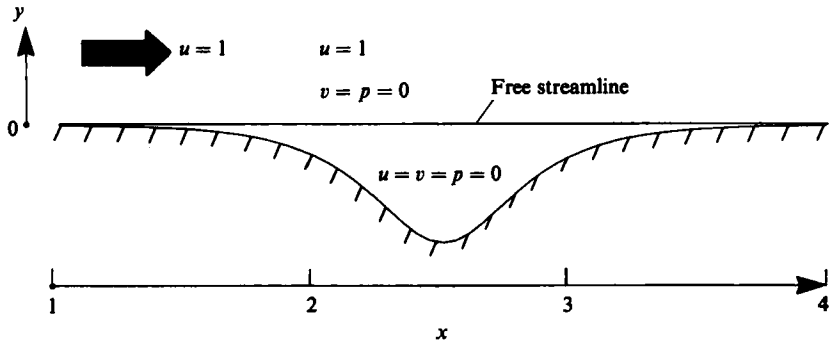

FIGURE 1. Kirchhoff free-streamline solution.

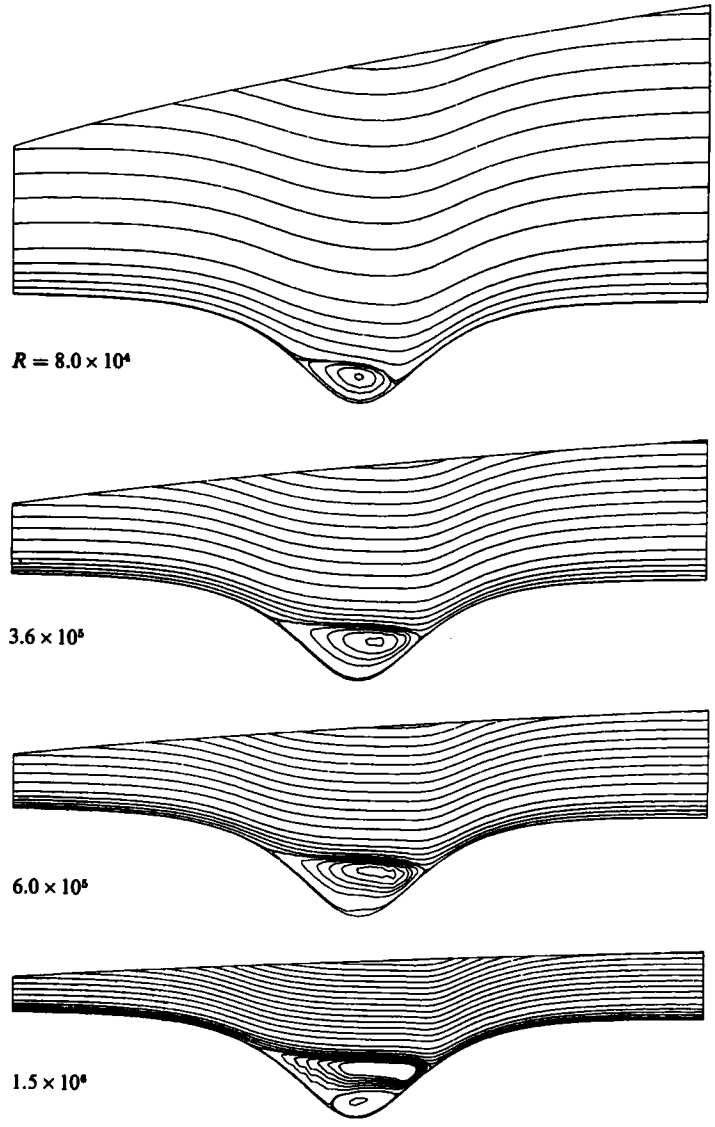

FIGURE 2. Streamlines of steady interacting boundary-layer solution along an indented plate.

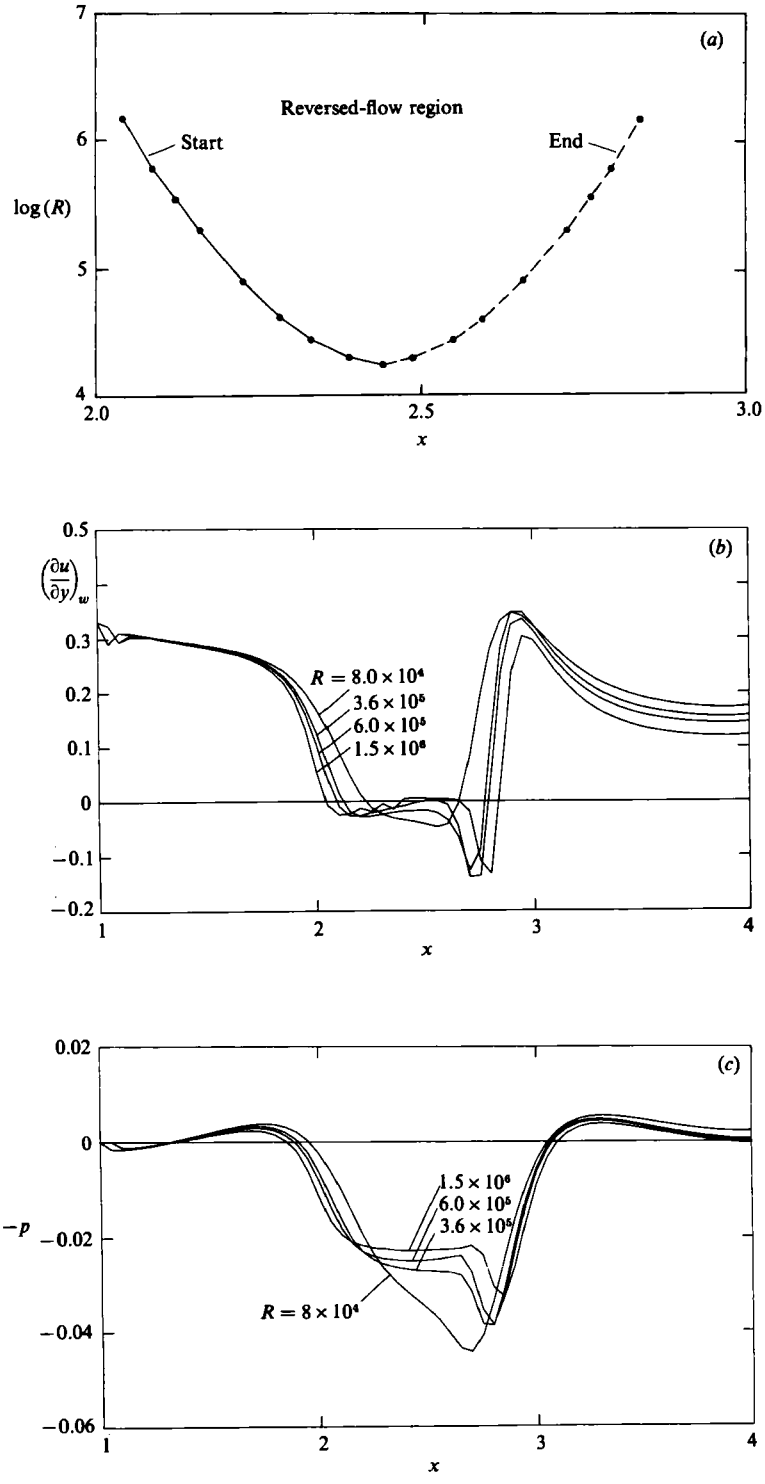

FIGURE 3(*a–c*). For caption see facing page.

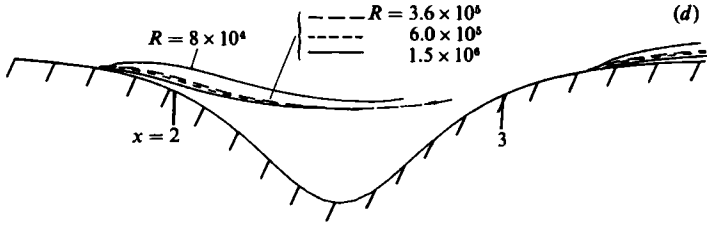

FIGURE 3. Detached-flow characteristics of steady interacting boundary-layer solution along indented plate. (*a*) Growth bubble; (*b*) wall shear stress; (*c*) pressure; (*d*) core of shear layer.

These results give the impression that, at this depth of the indentation, the interacting boundary-layer equations do have a steady solution at arbitrarily large Reynolds numbers. The difficulties encountered in the previous investigations seem to be of a numerical nature. This section is closed with some reflections on the physical meaning of the solution.

Steady classical boundary-layer solutions with edge velocity $u_{e,0}$ end up in a Goldstein singularity for indentations $\alpha < -0.0085$. Herwig (1981) suggests that the relevant Euler solution for indentations with such a Goldstein singularity is of the Kirchhoff free-streamline type, as depicted in figure 1. The steady interacting boundary-layer solution, being an attached boundary-layer strategy, supports the suggested detached boundary-layer structure, at least for the indentation $\alpha = -0.03$. Increase of the Reynolds number leads to a smooth transition from a steady attached flow to a steady detached flow, i.e. without any clear type of breakdown. The detached-flow characteristics in the steady interacting solution for increasing Reynolds number are summarized as follows:

(i) The recirculation region fills the indentation more and more (figure 3*a*).

(ii) The wall shear stress in the recirculation region tends to zero (figure 3*b*).

(iii) The pressure becomes constant in the recirculation region (pressure plateau), except close to the end of the recirculation region (figure 3*c*).

(iv) Viscous effects are more and more concentrated in a free shear layer. The core of the shear layer, where $(\partial u/\partial y)(x, y)$ reaches a maximum, approaches the shape of the suggested free streamline (figure 3*d*; near the end of the recirculation region the core of the shear layer is difficult to plot, and it is omitted in the figure).

It is seen that the second contribution to the edge velocity in (2) does not vanish for very large Reynolds numbers, but corrects the wrong choice of the relevant Euler solution $u_{e,0}$, which assumed an attached boundary layer in the limit $R \to \infty$. The interacting boundary-layer equations are not a true asymptotic description for the indentation $\alpha = -0.03$, because an asymptotic potential layer arises, for very large Reynolds numbers, between the free streamline and the wall, according to Herwig's detached flow model with finite-Reynolds-number effects, which is not captured in this composite formulation. The transition from the attached-flow description to the detached-flow description is smooth, implying that a range of Reynolds numbers exists where both descriptions are valid. Care must be taken with the interpretation of an attached-flow solution for a very large Reynolds number; the interacting boundary-layer equations for the indentation considered do not seem to warn of a special breakdown behaviour, although the solution has probably left the range of validity.

We have verified that the unsteady classical boundary-layer solution for the

indentation $\alpha = -0.03$ reveals a finite-time singularity of the Van Dommelen type (details are not presented here). The above results show that the interaction completely removes this singularity for the indentation considered; a steady-state limit of the unsteady equations can be obtained. In analogy with the analysis of the triple-deck equations by Stewartson *et al.*, it is expected that a critical combination of (α, R)-parameters exists, where a clear breakdown warning of the interacting boundary-layer solution is given: non-existence of the steady solution, with a finite-time singularity or the growth beyond all bounds for $t \to \infty$ in the unsteady solution. Instead of checking this for an indentation $\alpha < -0.03$, the unsteady interacting flow around the impulsively started cylinder is determined; its flow structure is believed to be comparable with the flow along the plate with indentation $|\alpha| = O(1)$.

4. Impulsively started cylinder

During recent years much interest has been given to the unsteady boundary-layer development around the impulsively started cylinder. Van Dommelen (1981) calculated very accurately that the unsteady classical boundary-layer solution develops a singularity within a finite time, implying the non-existence of a steady classical solution. The formation of this singularity has been confirmed by Cowley (1983) and Ingham (1984).

The cylinder configuration is depicted in figure 4. The characteristic velocity U_0 and length l are taken as two times the oncoming velocity, and the cylinder radius, respectively. The boundary condition $u = 0$ at $x = 0$ and π follows from the assumption that the flow is symmetric (for $x = \pi$ a boundary condition is only required for y-values that touch the region with backflow). $u_{e,0}$ is taken as $\sin x$, resulting from the Euler solution that assumes a symmetric potential flow with a vanishingly thin boundary layer along the wall. The first term in Blasius' (1908) series expansion for small times after the impulsive start is used to initiate the calculation at $t = 0.01$.

The unsteady classical boundary-layer calculation has been repeated. The implicit treatment of the x-derivatives in the backflow region requires some sweeps through the computational region; the convergence is very fast, and as a rule three sweeps are made at each time level. Calculated stream- and vorticity lines (81×41 spatial grid, with a timestep 0.01 for $0.01 \leqslant t \leqslant 0.1$ and 0.05 for $t > 0.1$) are shown in figure 5(*a*). The agreement with Van Dommelen (see the displacement thickness in figure 5*b*) is good until shortly before the appearance of the singularity at $t = 3.0045$. Comparison with our results on coarser grids ($21 \times 11, 41 \times 21$) showed that a much finer spatial grid, with a very small timestep, should be introduced after $t = 2.8$ to capture this singular growth. The wiggles in figure 5(*b*) are due to this lack of numerical resolution.†

Unsteady interacting boundary-layer solutions have been generated for $R = 10^6$, 10^5 and 10^4. One has to realize that only a simple interaction model is used, in which the effect of the finite cylinder curvature, for example, is neglected. x_e is chosen somewhat larger than π; the values of $u_e \delta^*$ for $x > \pi$ follow from the fact that $u_e \delta^*$ is an odd function around $x = \pi$ when symmetry is assumed. Calculated stream- and vorticity lines for $R = 10^6$ (41×21 spatial grid, with a timestep 0.01 for

† The results disagree with recent calculations of Cebeci (1986), suggesting that the singularity does not appear within a finite time. Deviations are already large at $t = 2.5$.

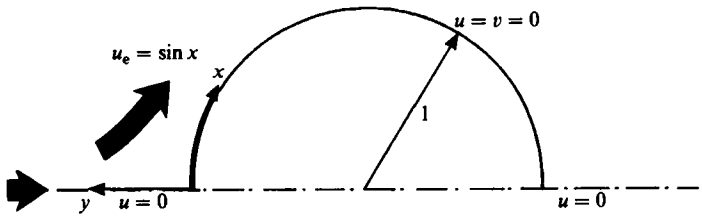

FIGURE 4. Impulsively started cylinder.

$0.01 \leqslant t \leqslant 0.1$ and a timestep 0.1 for $t > 0.1$; and an 81×41 spatial grid, with a timestep 0.01 for $0.01 \leqslant t \leqslant 0.1$, a timestep 0.1 for $0.1 < t \leqslant 2.5$ and a timestep 0.05 for $t > 2.5$) are depicted in figure 6(*a*) and the displacement thickness is shown in figure 6(*b*). It is seen that the recirculation region splits up into a lot of eddies at $t = 2.9$, all turning in the same direction. Stream- and vorticity lines and the displacement thickness for $R = 10^5$ are depicted in figures 7(*a*, and *b*) (again for a 41×21 and 81×41 grid). At $t = 2.7$ two peaks are formed in the displacement thickness, corresponding to the individualization of a vortex within the recirculation region. The grid size and timestep used are too coarse to decide whether the growth of the displacement thickness for $R = 10^5$ is singular at a finite time, or only leads to an unbounded solution for $t \to \infty$.

The oscillations in figures 6(*b*) and 7(*b*) are not ordinary numerical point-to-point wiggles. For instance, on the 81×41 grid, 6 intervals lie between the maximum and minimum in the displacement thickness in figure 7(*b*). Deviations between the solutions on the fine and coarser grids are small; smaller for $R = 10^5$ than for $R = 10^6$. The global pattern is believed to be physical. Moreover, the breakdown of the unsteady interacting boundary-layer solution seems to be similar to the breakdown of Smith's unsteady triple-deck solution for an ellipse with leading-edge bubble, as mentioned in the Introduction, showing both the same splitting up into eddies and the oscillations in the displacement thickness. Also there is a similarity with a recent study of Tutty & Cowley (1986), who show that a linear Rayleigh instability can develop in an unsteady triple-deck solution, leading to the formation of a series of eddies. It would be worthwhile to check whether the present unsteady solution of the interacting boundary-layer equations (for example at $t = 2.5$) is Rayleigh-unstable, initiating the breakdown. The similarity of the present results with the study of Smith on the one hand and Tutty & Cowley on the other hand poses the interesting question of a common physical mechanism.

Navier–Stokes solutions for $R = 10^5$ and 10^6 are unknown to the present authors. Comparison in figure 8 of the interacting boundary-layer solution at $R = 10^4$ with the Navier–Stokes solution of Dennis & Staniforth (1971) (a more extended calculation was recently given by Ta Phuoc Loc & Bouard 1985) shows a good agreement of the wall shear stress at $t = 0.6$ and 2.0, but there is only qualitative agreement at $t = 3.0$. One has to realize that the boundary layer is probably too thick for the interaction model to be accurate. Nevertheless, the interacting solution gives a better approximation of the Navier–Stokes solution than the classical solution. Experimental studies are only known up to $R = 10^4$ as well. Qualitative agreement is found between the interacting solution for $R = 10^5$ and the experiments of Bouard & Coutanceau (1980) for $R = 10^4$; in particular the individualization of a vortex, absent in the classical solution, is indeed captured in the interacting solution.

It is concluded that the interacting boundary-layer approach for the impulsively

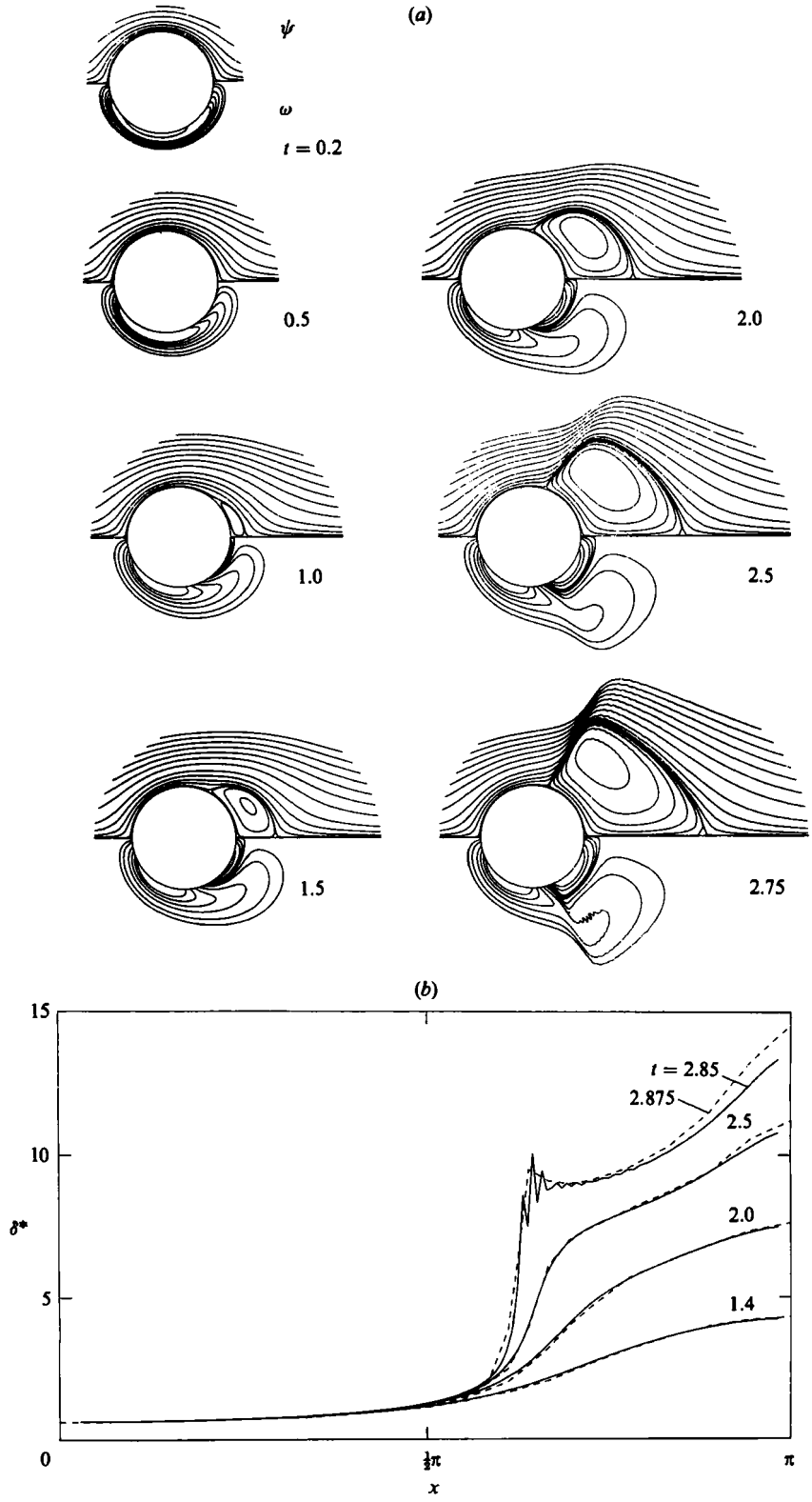

FIGURE 5. Classical boundary-layer solution for cylinder. (*a*) Stream- and vorticity lines (an extremely thick boundary layer is shown); (*b*) displacement thickness: ——, present; – – – –, Van Dommelen (1981).

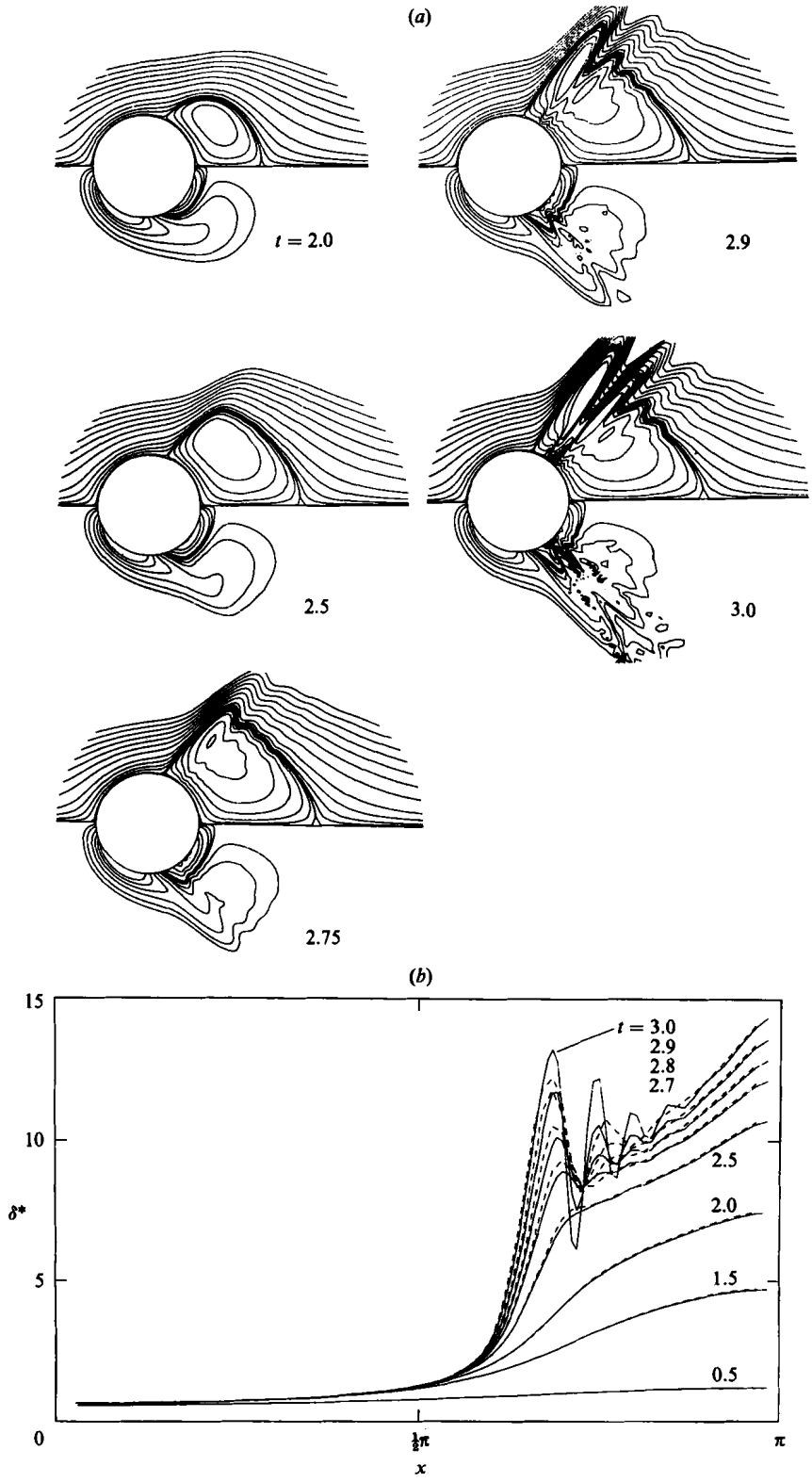

FIGURE 6. Interacting boundary layer of cylinder for $R = 10^6$. (*a*) Stream- and vorticity lines (radial coordinate of flow field is stretched with respect to cylinder radius); (*b*) displacement thickness: ——, $81 \times 41, \Delta t = 0.05$; – – – –, $41 \times 21, \Delta t = 0.1$.

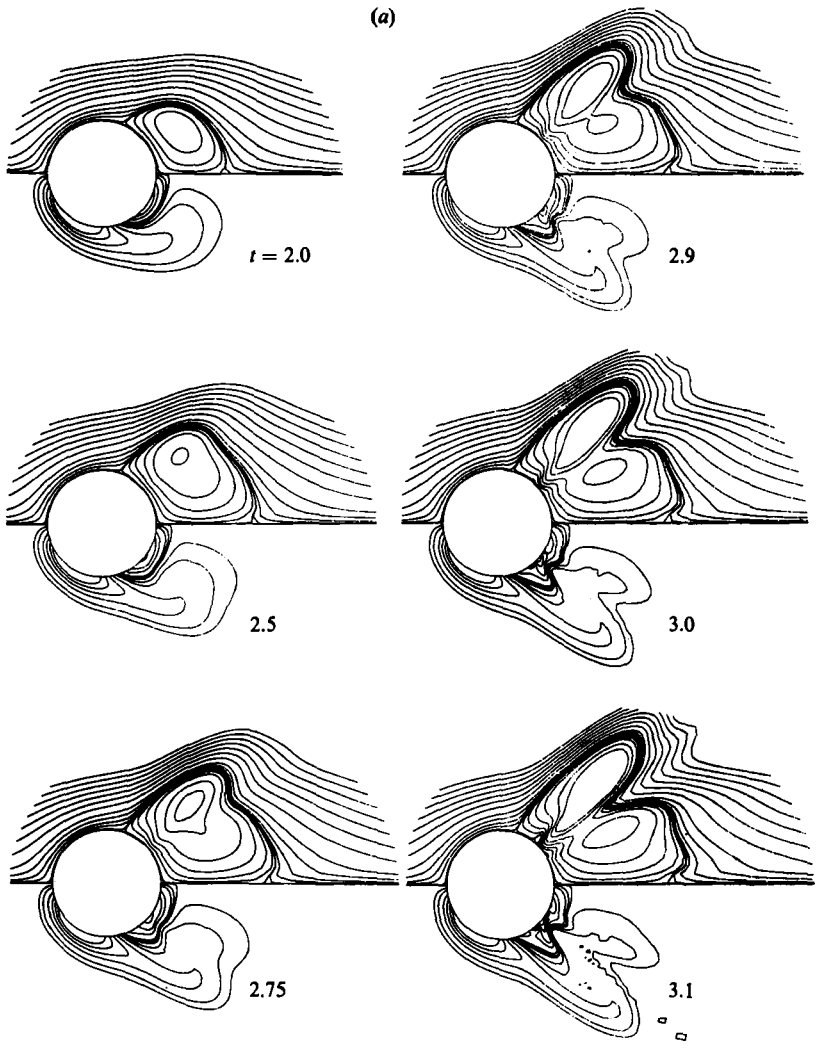

FIGURE 7(a). For caption see facing page.

started cylinder does at least delay the appearance of the finite-time singularity. However, the unsteady interacting solution is unbounded and a steady interacting solution does not exist. Van Dommelen's suggestion that the singularity in the unsteady classical solution corresponds to the individualization of a vortex in the experiments of Bouard & Coutanceau is strengthened by the interacting results for $R = 10^5$. The results also support the idea (Van Dommelen 1981; Smith 1982) that the singularity in the unsteady classical solution is the mathematical representation of an infinitely fast-growing vortex in the y-direction in the limit $R \to \infty$, indicating an *abrupt* transition from an unsteady attached to an unsteady detached flow. The interacting solution for a finite Reynolds number calculates the initial phase of the vortex growth (perhaps ending in a singularity), achieving a *violently unsteady* transition to the unsteady detached-flow structure (dynamic stall). When the vortex becomes too large, the attached interacting boundary-layer approach loses its validity; new asymptotic structures have to be developed to describe the unsteady detached continuation of the flow.

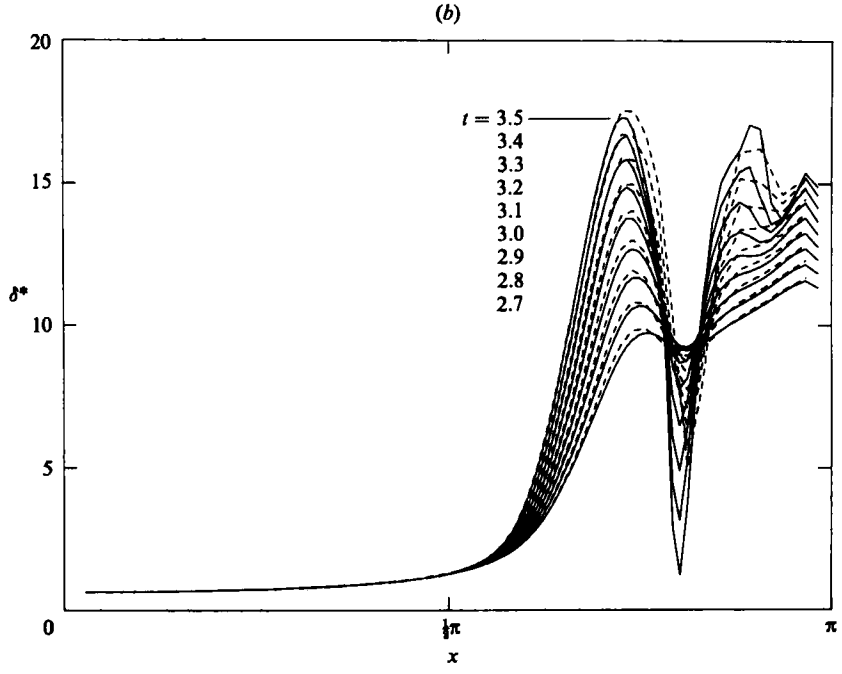

FIGURE 7. Interacting boundary layer of cylinder for $R = 10^5$. (*a*) Stream- and vorticity lines (radial coordinate of flow field is stretched with respect to cylinder radius); (*b*) displacement thickness: ——, $81 \times 41, \Delta t = 0.05$; – – – –, $41 \times 21, \Delta t = 0.1$.

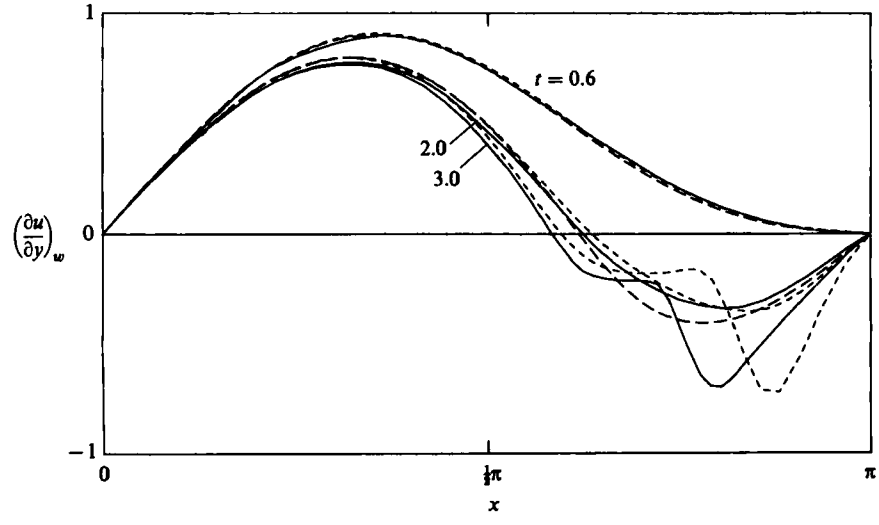

FIGURE 8. Boundary-layer solution of cylinder for $R = 10^4$ compared with Navier–Stokes solution: ——, Navier–Stokes solution (Dennis & Staniforth 1971); – – – –, interacting boundary-layer solution; — — —, classical boundary-layer solution.

5. Conclusion

For very small plate indentations ($-0.0085 \leqslant \alpha \leqslant 0$) the steady classical boundary-layer solution does not break down with a Goldstein singularity; the boundary layer remains attached, even in the limit $R \to \infty$. Interaction for the indentation $\alpha = -0.03$ removes the Goldstein singularity. An unsteady evolution prevents the numerical instabilities that were found in earlier calculations of steady solutions at very large Reynolds numbers. Increase of the Reynolds number leads to a smooth transition from a steady attached flow (viscous effects are only felt in an $O(R^{-\frac{1}{2}})$ layer close to the wall) to a steady detached flow (viscous effects are also felt in layers further removed from the wall), although the interacting boundary-layer solution for very large Reynolds numbers is not expected to capture the potential core of the detached flow; there may be a breakdown without any warning.

Interaction does delay Van Dommelen's finite-time singularity in the unsteady classical solution for the impulsively started cylinder, and further analysis is required to decide whether its appearance is totally prevented. The unsteady solution is unbounded, and hence a steady interacting solution does not exist. The individualization of a rapidly growing vortex in the interacting solution for $R = 10^5$, also found in experiments for $R = 10^4$, supports the idea that the breakdown of the classical and interacting cylinder solution refers to a sudden transition from an unsteady attached to an unsteady detached flow.

The two examples of boundary-layer flow discussed in this paper both feature Goldstein's singularity (in case of steady flow) and Van Dommelen's singularity (in case of unsteady flow) when the classical boundary-layer equations are solved. The addition of interaction leads to a different response in the two examples, which is related to the (non)existence of a steady solution. This different response of the interacting boundary-layer equations is in agreement with the asymptotic theory of Stewartson *et al.* and Smith, in which a critical combination of parameters appears, beyond which a steady solution ceases to exist.

The paper describes research performed in partial fulfilment of the engineering degree of one of the authors (R.A.W.M.H.) at the Department of Aerospace Engineering in Delft, under the responsibility of Professor J. L. van Ingen. The authors would like to thank him for his interest in this investigation.

REFERENCES

Blasius, H. 1908 Grenzschichten in Flüssigkeiten mit kleiner Reibung. *Z. angew. Math. Phys.* **56**, 1–37.

Bouard, R. & Coutanceau, M. 1980 The early stage of development of the wake behind an impulsively started cylinder for $40 < Re < 10^4$. *J. Fluid Mech.* **101**, 583–607.

Briley, W. R. & McDonald, H. 1975 Numerical prediction of incompressible separation bubbles. *J. Fluid Mech.* **69**, 631–656.

Brodetski, S. 1923 Discontinuous fluid motion past circular and elliptic cylinders. *Proc. R. Soc. Lond.* A **102**, 542–553.

Carter, J. E. & Wornom, S. F. 1975 Solutions for incompressible separated boundary layers including viscous–inviscid interaction. *Aerodynamic analyses requiring advanced computers*, part 1, *NASA SP* 347, pp. 125–150.

Cebeci, T. 1986 Unsteady boundary layers with an intelligent numerical scheme. *J. Fluid Mech.* **163**, 129–140.

COWLEY, S. J. 1983 Computer extension and analytic continuation of Blasius' expansion for impulsive flow past a circular cylinder. *J. Fluid Mech.* **135**, 389–405.

DENNIS, S. C. R. & STANIFORTH, A. N. 1971 A numerical method for calculating the initial flow past a cylinder in a viscous fluid. In *Proc. 2nd Intl Conf. Num. Meth. Fluid Dyn.* Lecture Notes in Physics, vol. 8, pp. 343–349. Springer.

DIJKSTRA, D. 1979 Separating, incompressible, laminar boundary-layer flow over a smooth step of small height. In *Proc. 6th Intl Conf. Num. Meth. Fluid Dyn.* Lectures Notes in Physics, vol. 90, pp. 169–176. Springer.

EDWARDS, D. E. & CARTER, J. E. 1985 A quasi-simultaneous finite difference approach for strongly interacting flow. In *Proc. 3rd Symp. on Numerical and Physical Aspects of Aerodynamic Flows, Long Beach, California, January 21–24.*

GOLDSTEIN, S. 1948 On laminar boundary-layer flow near a position of separation. *Q. J. Mech. Appl. Maths* **1**, 43–69.

HENKES, R. A. W. M. 1985 Computation of the separation of steady and unsteady, incompressible, laminar boundary layers. Engineering thesis, Report LR-483, Delft University of Technology, Department of Aerospace Engineering.

HERWIG, H. 1981 Die Anwendung der Methode der angepassten asymptotischen Entwicklungen auf laminare, zweidimensionale Strömungen mit endlichen Ablösegebieten. Dissertation, Ruhr-Universität, Bochum.

INGHAM, D. B. 1984 Unsteady separation. *J. Comp. Phys.* **53**, 90–99.

PRANDTL, L. 1904 Über Flüssigkeitsbewegung bei sehr kleiner Reibung. In *Proc. 3rd Intl Math. Congr., Heidelberg*, pp. 484–491.

ROTHMAYER, A. P. & DAVIS, R. T. 1985 Massive separation and dynamic stall on a cusped trailing-edge airfoil. In *Proc. 3rd Symp. on Numerical and Physical Aspects of Aerodynamic Flows, Long Beach, California, January 21–24.*

SMITH, F. T. 1977 The laminar separation of an incompressible fluid streaming past a smooth surface. *Proc. R. Soc. Lond.* A **356**, 443–463.

SMITH, F. T. 1979 Laminar flow of an incompressible flow past a bluff body: the separation, reattachment, eddy properties and drag. *J. Fluid Mech.* **92**, 171–205.

SMITH, F. T. 1982 Concerning dynamic stall. *Aero. Q.* **33**, 331–351.

STEWARTSON, K., SMITH, F. T. & KAUPS, K. 1982 Marginal separation. *Stud. Appl. Math.* **67**, 45–61.

SYCHEV, V. V. 1972 Concerning laminar separation. *Izv. Akad. Nauk. SSSR Mekh. Zhid. i Gaza* **3**, 47–59 (in Russian). (English translation *Fluid Dyn.* **7**, 407–417.)

TA PHUOC LOC & BOUARD, R. 1985 Numerical solution of the early stage of the unsteady viscous flow around a circular cylinder: a comparison with experimental visualization and measurements. *J. Fluid Mech.* **160**, 93–117.

TUTTY, O. R. & COWLEY, S. J. 1986 On the stability and the numerical solution of the unsteady interactive boundary-layer equation. *J. Fluid Mech.* **168**, 431–456.

VAN DOMMELEN, L. L. 1981 Unsteady boundary layer separation. Ph.D. thesis, Cornell University, New York.

VELDMAN, A. E. P. 1979 A numerical method for the calculation of laminar, incompressible boundary layers with strong viscous–inviscid interaction. *NLR TR* 79023U.

VELDMAN, A. E. P. 1981 New, quasi-simultaneous method to calculate interacting boundary layers. *AIAA J.* **19**, 79–85.

VELDMAN, A. E. P. & DIJKSTRA, D. 1980 A fast method to solve incompressible boundary-layer interaction problems. In *Proc. 7th Intl Conf. Num. Meth. Fluid Dyn.* Lecture Notes in Physics, vol. 141, pp. 411–416. Springer.